Journal of Applied Pharmaceutical Science Vol. 13(04), pp 141-148, April, 2023
Available online at http://www.japsonline.com
DOI: 10.7324/JAPS.2023.41561
ISSN 2231-3354

Chitosan-tripolyphosphate nanoparticles encapsulated rutin targeting bacterial growth inhibition and its cytotoxicity on PANC-1 pancreatic adenocarcinoma cell

K. T. Ramya Devi*, Shalini James Paulraj, Yashesh Shah, Santhosh Raja Kumar, Priyatharcini Kejamurthy
Department of Biotechnology, School of Bioengineering, SRM Institute of Science and Technology, Kattankulathur, India.

ARTICLE INFO

Received on: 18/08/2022
Accepted on: 31/12/2022
Available Online: 28/03/2023

Key words:
Chitosan, rutin, PANC-1, C3H10T1/2, tripolyphosphate, pancreatic cancer.

ABSTRACT

Nano-carrier systems are highly explored for the slow release of a drug. Chitosan (CS), a polymer, has more applications in nano-drug carrier systems. To explore these applications, currently, we synthesized CS nanoparticles (CS-NPs), and it was allowed to encapsulate free Rutin (RUT) and it resulting in CS-NPs/RUT. Further, it was characterized, and the size of CS-NPs was found to be 79 nm, and upon encapsulating RUT, the particle size was increased to 173 nm, which resulted in CS-NPs/RUT. The entrapment of RUT with CS-NPs was found to be -85%. MTT-based cytotoxicity assay represented the non-lethal nature of CS-NPs/RUT toward normal osteoblast cells, C3H10T1/2 clone8, and showed cytotoxicity against pancreatic adenocarcinoma cells, PANC-1. Furthermore, we extended the study to analyze bacterial growth inhibition and incorporation by CS-encapsulated RUT. It was performed through flow cytometry in different concentrations of 100, 200, and 300 µg/ml of treatments in *Escherichia coli*. The bacterial inhibition and incorporation of bacteria were significantly higher in CS-NPs/RUT compared with RUT. Hence, the experiments depicted the superiority of CS-NPs/RUT over free RUT that suggested, CS encapsulation as an efficient system for delivering RUT for bacterial growth inhibition and also anti-cancer cell proliferation.

INTRODUCTION

Chitosan (CS), also known as deacetylated chitin, is distributed promiscuously as a polymer (Anitha *et al*., 2014). CS possesses distinct properties like bioactivity, nontoxicity, biodegradability, mucoadhesion, and biocompatibility (Vernaez *et al*., 2019). It has been used widely for delivering various therapeutic drugs because of its ideal properties (Mohammed *et al*., 2017). Nanoencapsulation enhances the specificity, targeting ability, and efficacy of the polymers used in the drug delivery system. CS nanoparticles (CS-NPs) are widely used as drug carriers (Raza *et al*., 2020). Tripolyphosphate (TPP) has multiple attachment sites and can be used as a crosslinker for CS. TPP is a polyanion that interacts with CS (cationic), employing electrostatic forces (Pan *et al*., 2020). TPP has been physically endorsed to crosslink CS for biomedical purposes through ionic gelation. The US Food and Drug Administration has accepted TPP as an unobjectionable food additive (Pan *et al*., 2020). Producing CS nanoparticles includes emulsion solvent diffusion, reverse micellar method, desolvation, ionic gelation, emulsion droplet coalescence, and polyelectrolyte complexion (Naskar *et al*., 2018). Oxidative stress could be a condition where the antioxidant defense mechanism in cells becomes inadequate, leading to the excess production of reactive oxygen species (ROS) or inactivation of ROS and damaging sugars, lipids, and DNA (Waris and Ahsan, 2006). Flavonoids are polyphenolic compounds that induce apoptosis, inhibit angiogenesis, disrupt mitotic spindle formation, and block the cell cycle. It makes them acceptable agents in cancer biology (Panche *et al*., 2016). Flavonoids have significant antioxidant properties for scavenging free radicals, which cause tumor promotion and

*Corresponding Author
K. T. Ramya Devi, Department of Biotechnology, School of Bioengineering, SRM Institute of Science and Technology, Kattankulathur, India.
E-mail: ramyakanth3 @ gmail.com

cell damage (Kopustinskiene *et al*., 2020). Flavonoids suppress the growth of cell tumors which is mediated by the triggering apoptosis in numerous cancer cells and various types of cell cycle prevention (Zhang *et al*., 2012). RUT is a naturally occurring flavonoid and is distributed in many plants (Devi *et al*., 2018). Rutin (RUT) is a hydrophobic polyphenolic flavonoid with enounced chemopreventive properties against various cancers *in vivo* and *in vitro* (Ganeshpurkar and Saluja, 2017). RUT was extensively studied for its antimicrobial activity against various strains of bacteria such as *Escherichia coli*, *Pseudomonas aeruginosa*, *Bacillus subtilis*, *Proteus vulgaris*, *Shigella sonnei*, and *Klebsiella* species (Ganeshpurkar and Saluja, 2017). RUT has various valuable pharmacological properties, including anti-cancer, anti-inflammatory, neuroprotection, antimicrobial, anti-proliferative, anti-carcinogenic, and anti-oxidative stress effects (Imani *et al*., 2020). A recent study stated that the administration of RUT and other anti-cancer drugs reduced the side effects of chemotherapy and drug resistance against prostate, lung, colon, and breast cancer cells (Al-Rajhi *et al*., 2022). In addition, it modulated major transcription activators, namely, mitogen activated protein kinase, PI3K/Akt, and Janus kinase/signal transducers in carcinogenic cells (Satari *et al*., 2021).

Pancreatic cancer is a highly fatal malignant disease with an overall survival rate of 10% (at diagnosis) and others being affected with metastatic or unresectable disease (Brentjens and Saltz, 2001). Since RUT has anti-tumor and cytotoxic properties, it has been taken for the study. In this study, we have prepared and characterized CS-NPs loaded with RUT and determined the outcome of RUT released from CS-NPs/RUT on bacterial growth inhibition and its cytotoxicity on pancreatic ductal adenocarcinoma cells, PANC 1.

MATERIALS AND METHODS

Materials

CS, RUT, 3-(4, 5- dimethylthiazol-2yl)-2, 5-diphenyl tetrazolium bromide (MTT), and sodium TPP were purchased from Sigma Aldrich, USA. C3H10T1/2 clone8 cells and PANC1, pancreatic adenocarcinoma cells were obtained from National Centre for Cell Sciences, Pune, India. Minimum essential media and Dulbecco's Modified Eagle Medium (DMEM), and fetal bovine serum (FBS) were purchased from Thermo Scientific, USA. BrdU cell proliferation assay kit was procured from Calbiochem, CA.

Methods

CS-NPs and CS-NPs/RUT – preparation

CS-NPs were formulated as described by Li *et al.* (2016). A ratio of 2:1 and 5:1 of CS to TPP in 0.1, 0.3, and 0.5 mg/ml concentration of rutin (CS-NPs/RUT) were prepared. Further, characterization, bacterial growth inhibition, and cell proliferation were carried out. Experiments were designed with a treatment duration of 24 hours.

CS-NPs and CS-NPs/RUT – characterization

The shape particle size was analyzed through a scanning electron microscope (SEM), and also the charge and the particle size were analyzed by using a Zetasizer Nano Series instrument (Horiba Nano Partica SZ-100, Japan). To analyze the composition of the elements and functional groups in the CS-NPs and CS-NPs/RUT, energy dispersive spectroscopy (EDS) and Fourier-transformed infrared spectroscopy (FT-IR) were utilized, respectively.

Dynamic light scattering

The particle size of CS-NPs and CS-NPs/RUT were determined using a Zetasizer. The particles were suspended in distilled water and were stirred overnight at 250 rpm, and a serial dilution was made with water, then it was sonicated for a short period to break the aggregated particles. Later the particle size of the particle was determined. The polydispersity index (PdI) was determined by dividing the particle diameter distribution's standard deviation (σ) by the mean particle diameter.

Analysis of entrapment efficiency

It was experimented with to analyze the encapsulation efficiency (EE) of CS-NPs with RUT. The CS-NPs and CS-NPs/RUT were synthesized using the ionic gelation method. Carbon nanoparticles were generated by inducing the gelation of carbon dioxide solution with sodium TPP. Inotropic gelation occurs due to positively charged amino groups interacting with negatively charged TPP. Initially, CS was dissolved in aqueous solutions containing 1% acetic acid at room temperature for 20–24 hours in magnetic stirring until a clear solution was obtained. Two ratios of 2:1 and 5:1 ratio of CS-NPs to TPP were prepared. 0.1, 0.3, and 0.5 mg/ml of RUT concentration were prepared and added individually to each ratio of CS-NPs to TPP. Before preparing CS-NPs and CS-NPs/RUT, all solutions were filtered in a 0.22-micron filter.

CS-NPs were prepared by adding TPP solution dropwise to CS solution and were subjected to magnetic stirring at 500 rpm at room temperature. Similarly, CS-NPs/RUT was prepared similarly to CS-NPs along with RUT and trehalose. Trehalose (3 mg) to the CS solutions was added to avoid particle aggregation. The prepared CS-NPs and CS-NPs/RUT were centrifuged at 10,000 rpm for 30 minutes to remove residuals from CS particles during dispersion. The percentage of RUT incorporated by CS-NPs was measured in the supernatant obtained through centrifugation.

The ratio, 2:1 and 5:1 of CS-NPs to TPP, was prepared. 0.1, 0.3, and 0.5 mg/ml were the amount of RUT added individually in each ratio of CS-NPs to TPP. The percentage of RUT incorporated by CS-NPs was measured from the supernatant obtained during the synthesis of CS-NPs/RUT. The amount of RUT released in the supernatant during the encapsulation process would be inversely proportional to the concentration of RUT entrapped by CS-NPs. High-performance liquid chromatography (HPLC) was utilized for the analysis per the protocol that followed (Kumar *et al*., 2015). Among these two different ratios, the ratio that has actual particle size and the charge would be chosen for the study and analyzed for EE.

Bacterial growth inhibition – determination of bacterial incorporation and viability by flow cytometer

Escherichia coli, a gram-negative bacterium, was taken to experiment with reducing bacterial growth by CS-NPs/RUT. The bacteria were exposed to concentrations of CS-NPs/RUT

(100, 200, and 300 µg/ml) and compared with untreated control for bacterial inhibition. According to the protocol followed earlier (Sridevi *et al*., 2020), it was experimented with and analyzed by a flow cytometer BD FACSCalibur™

Cytotoxicity of CS-NPs/RUT on mammalian cell line

C3H10T1/2 clone 8, a mouse mesenchymal stem cell, and PANC1, pancreatic adenocarcinoma cells, were cultured with Minimal essential media and DMEM, respectively, supplemented with 10% FBS with 2 mM L-glutamine, 1 mM Sodium pyruvate, and 2.2 mM Sodium bicarbonate. The cells were maintained in an atmosphere containing 5% CO_2 at 37°C. 25, 50, and 75 µg/ml CS-NPs/RUT have been opted for the study.

Assessment of cell proliferation

Cell proliferation assay was carried out according to the manufacturer's procedure (Calbiochem, CA). According to the principle, the absorbance of BrdU incorporation into DNA (Wu *et al*., 2013) is directly proportional to the amount of DNA, and the absorbance was measured at 405 nm.

Cell cytotoxicity – formazan assay

The reduction of MTT to formazan crystal was measured to analyze metabolically viable cells using the method depicted by Madesh and Balasubramanian (1997). 1×10^4 C3H10T1/2 clone8 cells and PANC1 cells were allowed to adhere, and once it attained confluence, the treatment was performed with three different concentrations. The formazan crystals formed were solubilized using DMSO, and the absorbance was then measured using a microtiter plate reader at 570 nm.

Analysis of statistical significance

One-way analysis of variances was performed using Statistical Package for the Social Sciences software version 17.0 to determine the statistical significance of $p < 0.05$. All the experiments were performed with an "*n*" number in a group of three.

RESULTS

Particle size and charge analysis

The overall surface charges of the nanocomposites were estimated using zeta potential analysis. RUT exhibited a negative charge of −11 mV, while CS-NPs exhibited a positive charge of +10 mV. However, when RUT was incorporated into CS-NPs, the composite showed an overall positive surface charge of +3.64 mV. This shifting in the zeta potential toward positive value ascribes to favorable electrostatic interaction of the negatively charged functional groups of RUT, and the positively surface charged CS-NPs leading to the formation of a stable nanocomposite. The surface charge of the particles was determined by zeta potential and was found to be increased as the mass ratio increased from 2:1 to 5:1 for CS-NPs/RUT.

The PdI value of CS-NPs is 0.008 and CS-NPs/RUT is 0.006, which indicates that both PDI values are less than 0.2, which could be accepted in practice for polymer-based nanoparticle materials. SEM determined the particle shapes of the CS-NPs and CS-NPs/RUT represented in Figure 1. The average diameter of CS-NPs and CS-NPs/RUT was 79.6 ± 52.4 and 173 ± 29 nm. The size of the CS-NPs/RUT was larger than the CS-NPs, representing that CS-NPs have encapsulated RUT. Since CS and RUT have comparable hydrophobic properties, they were blended in the organic solvent, creating a strong affinity between them. CS-NPS encapsulated anti-cancer agents, proteins such as retinol (Kim *et al*., 2006), and antioxidants (Kumar *et al*., 2015). RUT was found to maintain its properties in an encapsulated form (Takahashi *et al*., 2020). Any encapsulated molecules can be easily absorbed by the system and have a high pharmacological effect.

Fourier transform infrared spectroscopy (FTIR)

The molecular interactions between CS-NPs and RUT have been studied by chemically analyzing their functional groups using FTIR spectrometry analysis (Das *et al*., 2013). The FTIR spectrum of CS-NP shows in ure 2a the characteristic sharp absorption bands at 3,317.63 cm^{-1} (O-H stretching), 1,395.74

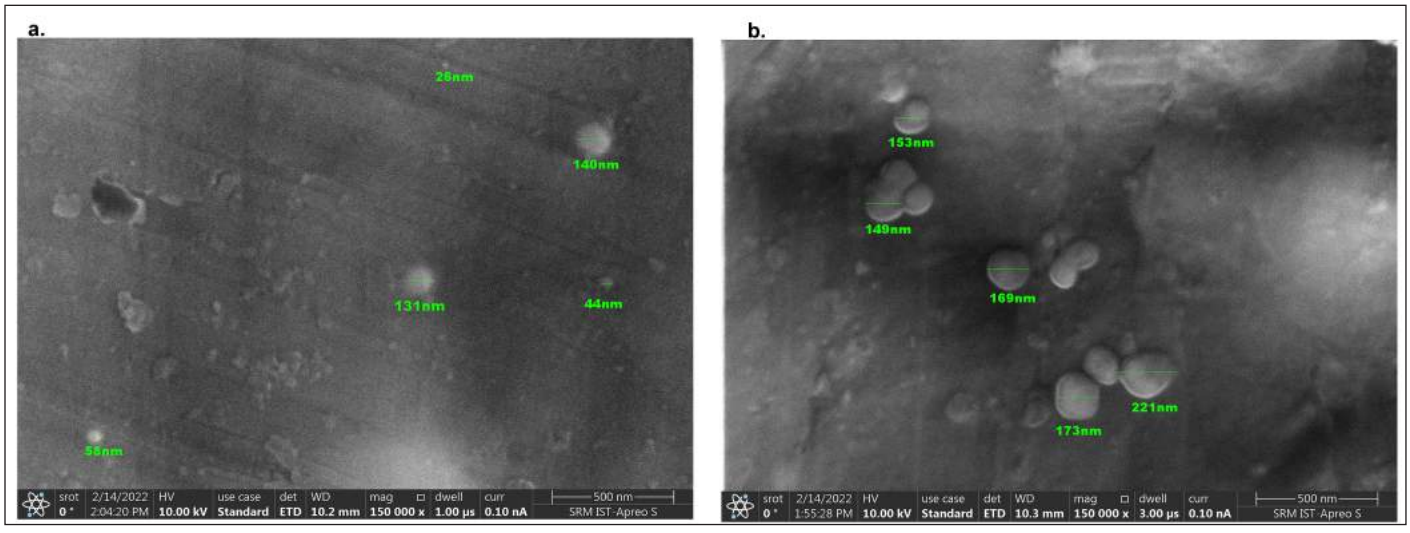

Figure 1. Field-Emission Scanning Electron Microscopy (FESEM) images of CS-NPs and CS-NPs/RUT.

cm^{-1} (O-H bending vibration), 1,116.39 cm^{-1} (C-O stretching), 752.13 cm^{-1} (NH out-of-plane bending), 604.97 cm^{-1} (overlap of out-of-plane C-O and NH bending), and weak absorption bands at 1,182.80 cm^{-1} (C-O-C stretching), 1,675.10 cm^{-1} (amide C=O stretching), and 2,354.91 cm^{-1} (C-N asymmetric band stretching). The IR spectra of pure RUT show characteristic peaks at 3,290.99 cm^{-1} (O-H bending), 2,830–3,100 cm^{-1} (CH 3 asymmetric stretching), 1,632.77 cm^{-1} (aryl ketone, C=O stretching), 1,501.74 cm^{-1} (C=C stretching), 1,308.49 cm^{-1} (O-H functional group), and 1,247.93 cm^{-1} and 1,061.20 cm^{-1} (C-O-C stretching) as mentioned at Figure 2b. In the case of CS-NPs/RUT shown in Figure 2c, the characteristic absorption spectra at 1,602.83 cm^{-1} correspond to the C=O stretching of RUT, thus affirming the successful incorporation of RUT in the CS-NPs. A noticeable shift of the O-H stretching band to 3,314.43 cm^{-1} was attributed to the interactions between CS-NPs and RUT via hydrogen bond formation, as observed in a previous analysis (Patil and Jobanputra, 2014).

Energy dispersive spectroscopy (EDS)

EDS is a highly used tool to identify the elemental composition of a compound. Different peaks were observed CS-NPs, RUT, and CS-NPs/RUT. Among these, CS-NPs/RUT was observed with more nitrogen, carbon, phosphorous, and oxygen than the others, all shown in Figure 3.

Entrapment efficiency (EE)

The entrapment efficiency RUT by CS-NPs was detected using HPLC with a UV detector. Among the two different CS is to TPP ratios, 5:1 had given definite particle size and charge; hence, it was chosen for further analysis. The supernatant obtained during the preparation of CS-NPs/RUT in three different concentrations of RUT, 0.1 mg, 0.3 mg, and 0.5 mg/ml, was used as a sample in HPLC. As experimented, EE was observed higher with the high concentration of RUT loaded in the higher ratio, 5:1 of CS: TPP. The percentage EE obtained for 0.1 mg, 0.3 mg, and 0.5 mg/ml of RUT obtained an efficiency of approximately 13%, 67%, and 85%, respectively. The result suggests that higher entrapment of RUT was obtained in 0.5 mg/ml of RUT, so high encapsulation could be attained by loading 0.5 mg/ml of RUT in a 5:1 ratio of CS to TPP. And so, the result reveals that the encapsulation system is efficient in loading RUT into CS-NPs.

In earlier studies, RUT has been estimated to be a potential flavonoid acquiring many pharmacological and

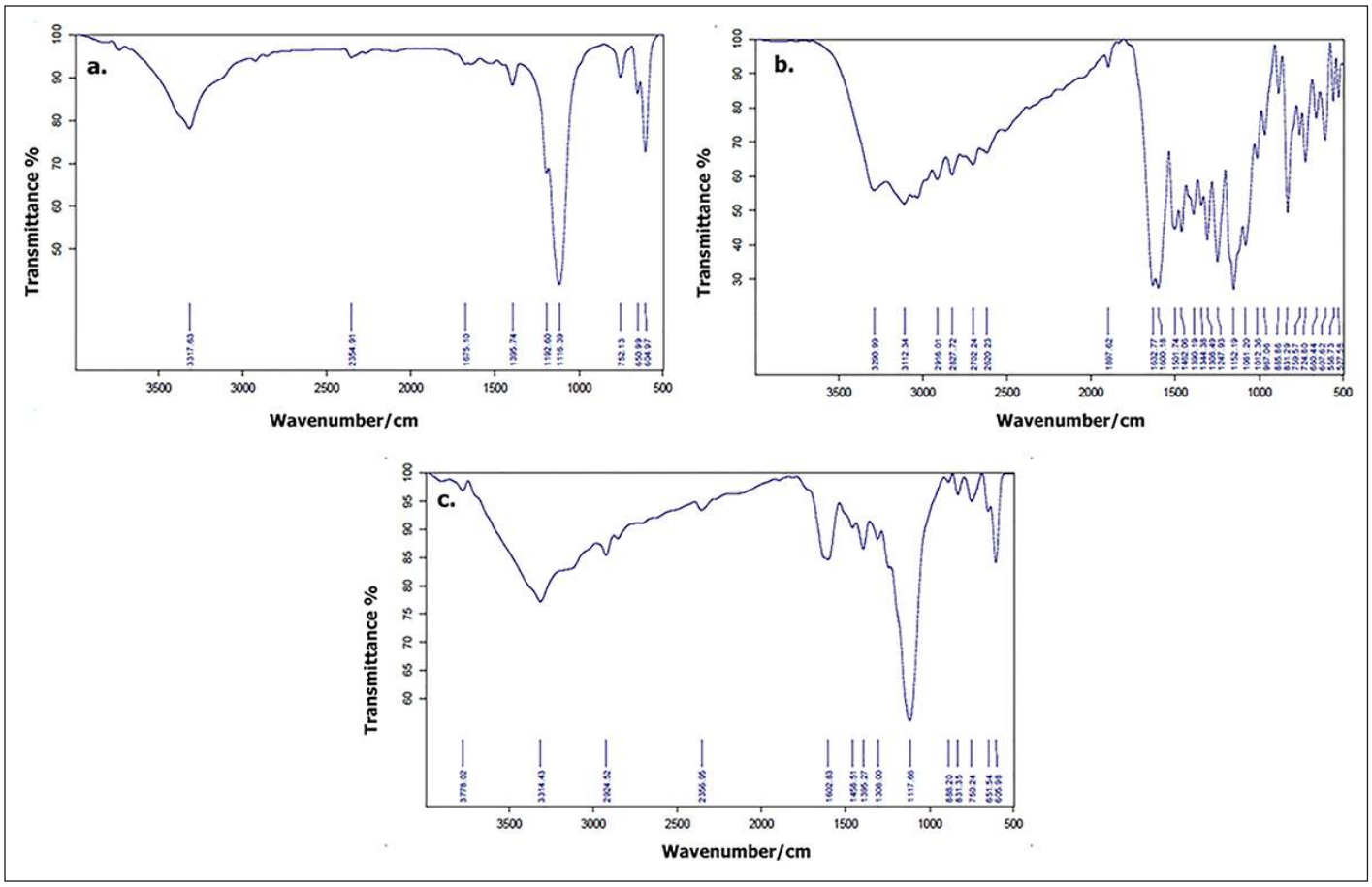

Figure 2. FT-IR spectra of (a) CS (b) CS-NPs and (c) CS-NPs/RUT.

biological properties. RUT acts as a free radical scavenger and scavenges that could probably protect normal cells. It also has a prominent role in maintaining the development and programmed cell death of uncontrolled growth of cells (Perk *et al*., 2014). It has been proclaimed that free radicals are one of the activators for higher diseases and disorders (Lobo *et al*., 2010). Thus, enhanced free radical production induced both extrinsic and intrinsic programmed cell death in cancer cells (Sharma *et al*., 2019).

Cell cytotoxicity studies

The cytotoxicity of C3H10T1/2 clone 8 and PANC1 cells concerning CS-NPs/RUT can be influenced by mitochondrial dehydrogenase activity. When the normal osteoblast cell, C3H10T1/2 clone8, was exposed to CS-NPs, RUT, and CS-NPs/RUT, there was a significant decline in the viability of cells in comparison to untreated c (Fig. 4). Among other groups, the cell viability percentage was maintained in CS-NPs/RUT, and also there was a significant decrease in the cell count observed in all groups.

In the case of treatment with the pancreatic cancer cell, PANC1, the cell cytotoxicity seems to be enhanced when treated with different concentrations of CS-NPs/RUT as the concentration increases compared to the untreated control. It resulted in low mitochondrial dehydrogenase activity in the group treated with a high concentration of CS-NPs/RUT. The above results imply that treatment with a high concentration of 0.5 mg/ml of CS-NPs/RUT has shown more cytotoxicity against PANC1 cells, as shown in Figure 5.

Cell proliferation assay

BrdU, a thymidine analog, gets incorporated into the newly synthesized DNA during replication. This criterion has been used for the PANC1 cell proliferation analysis. A very low absorbance was spotted in the group exposed to CS-NPs/RUT compared with the untreated group treated with RUT. It has

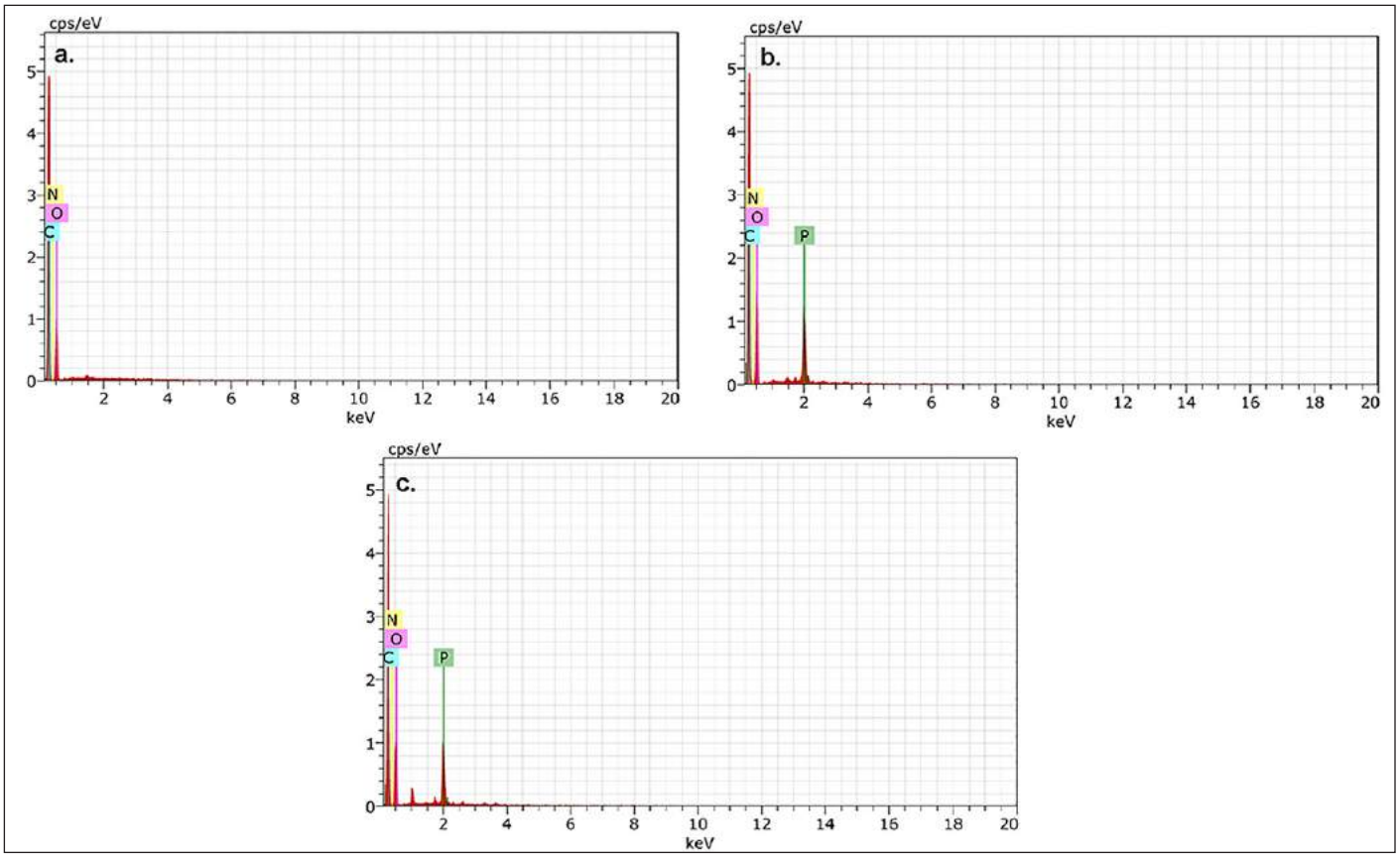

Figure 3. EDS spectra of (a) CS (b) CS-NPs and (c) CS-NPs/RUT.

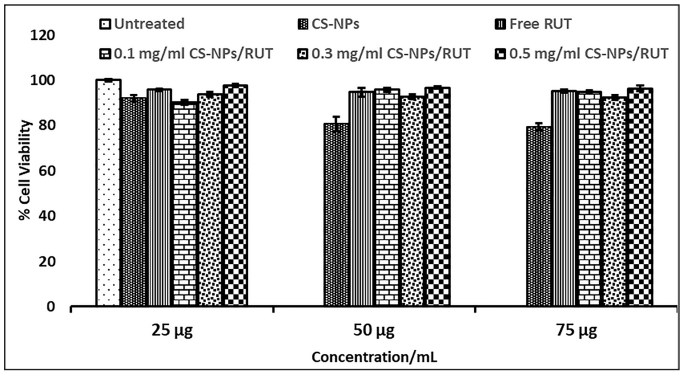

Figure 4. Determination of cytotoxicity of encapsulated Rutin on Normal C3H10T1/2 clone 8 cells by MTT formazan assay.

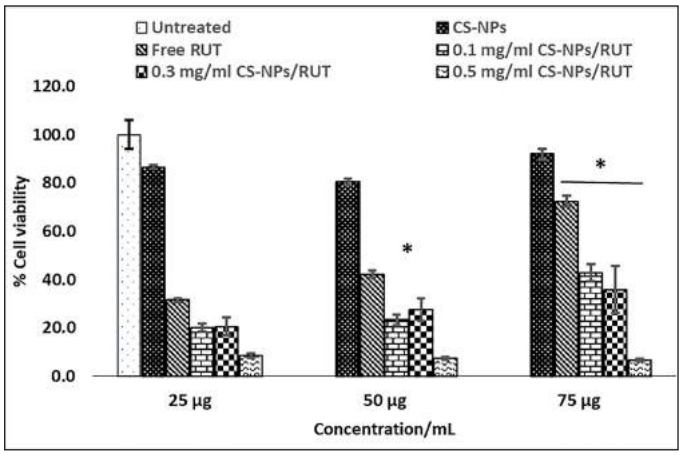

Figure 5. Determination of cytotoxicity of encapsulated Rutin on PANC1 pancreatic cancer cell by MTT formazan assay. * Represents groups significant ($p < 0.05$) when compared to 25, 50, and 75 µg of untreated control in their respective concentration, and # represents groups significant ($p < 0.05$) when compared to 25 µg, 50 µg, and 75 µg/ml of free rutin in their respective concentration.

represented in Figure 6, and these results imply that CS-NPs/RUT can reduce the proliferation of PANC1 cells.

Studies on the incorporation of bacteria using flow cytometry

An untreated control was weighed with the groups treated with maximum concentration, i.e., 75 µg/ml of CS-NPs, RUT, and CS-NPs/RUT. The dot blots given by the flow cytometry system were included for the examination and further adopted the gating strategy and are represented in Figure 7. The dot plot was gated into R1 (background region), R2 (live-cell region), and R3 (incorporated cell region) regions based on the different populations and the scatter pattern. The percentage incorporation of RUT was calculated based on the dot plot data. The incorporation of bacteria by CS-NPs/RUT was taken from the R3 region and calculated. There was an augmentation in the incorporation of bacteria in the group treated with a high concentration of 0.5 mg/ml CS-NPs/RUT compared with the untreated CS-NPs, and RUT.

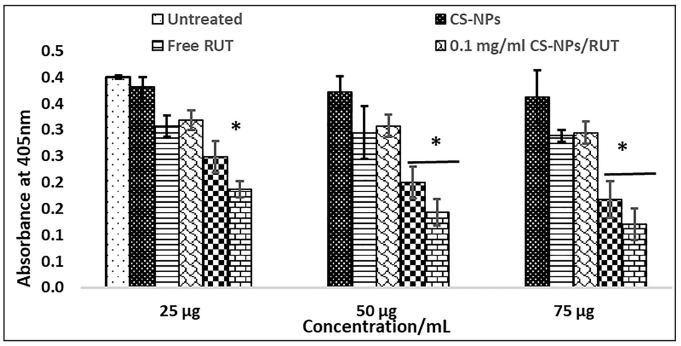

Figure 6. Encapsulated Rutin determined PANC1 pancreatic cancer cell proliferation by BrdU cell proliferation assay. * Represents groups significant ($p < 0.05$) when compared to 25 µg, 50 µg, and 75 µg of untreated control in their respective concentration, and # represents groups significant ($p < 0.05$) when compared to 25 µg, 50 µg, and 75 µg/ml of free rutin in their respective concentration.

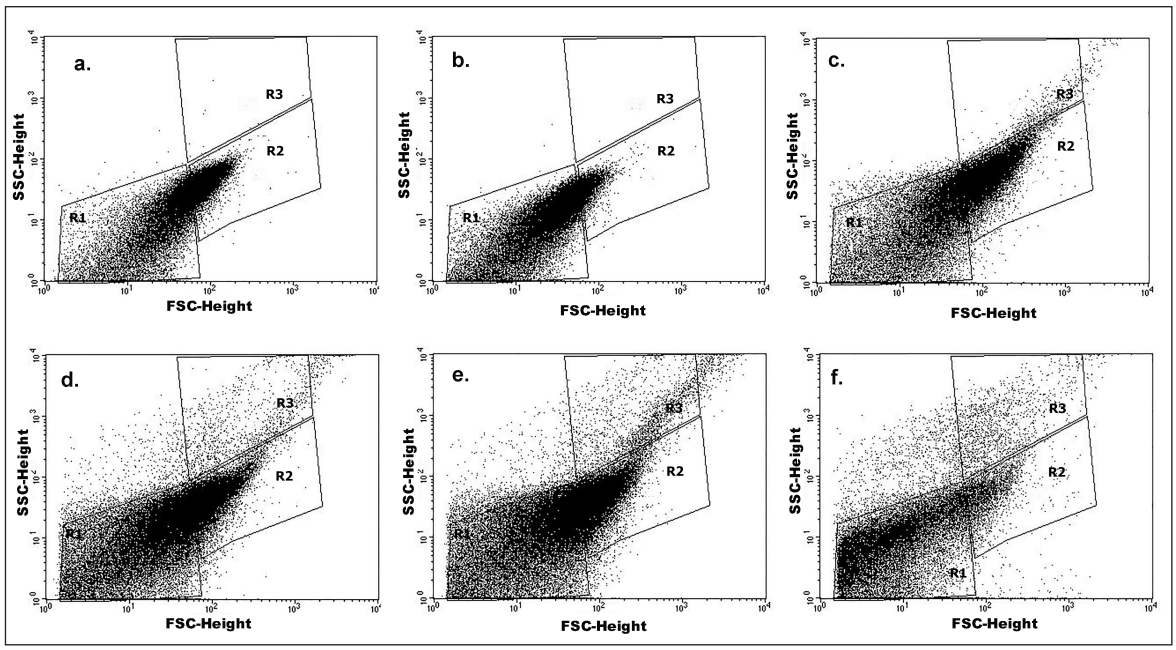

Figure 7. Effect of CS-NPs, free RUT, and CS-NPs/RUT on *E. coli* cell growth inhibition. Figures a–f is a representation of the dot plot of flow cytometry analysis with a side scatter height and a forward scatter height for the groups (a) untreated, (b) CS-NPs treated, (c) Free RUT treated, (d) 0.1 mg/ml CS-NPs/RUT treated, (e) 0.3 mg/ml CS-NPs/RUT treated, and (f) 0.5 mg/ml CS-NPs/RUT treated.

CONCLUSION

The generated CS-NPs/RUT, 5:1 mass ratio of CS:TPP was examined as optimal. And it has a great entrapment efficiency that was confirmed with HPLC. The steadiness of CS-NPs/RUT was analyzed using EDS, SEM, and FTIR. The CS-NPs/RUT particles were found to be spherical. CS-NPs/RUT has efficient cytotoxicity toward PANC1 cells, which were examined using a formazan assay. Also, the proliferation of the same can be reduced by it. Additionally, bacterial inhibition studies state that it enhances bacterial incorporation of particles. Hence, CS-NPs/RUT can be utilized as an effective carrier in the drug delivery system.

AUTHOR CONTRIBUTIONS

All authors made substantial contributions to conception and design, acquisition of data, or analysis and interpretation of data; took part in drafting the article or revising it critically for important intellectual content; agreed to submit to the current journal; gave final approval of the version to be published; and agree to be accountable for all aspects of the work. All the authors are eligible to be an author as per the international committee of medical journal editors (ICMJE) requirements/guidelines.

FINANCIAL SUPPORT

This manuscript received financial support from the National Symposium on "Emerging Innovations in Applied Biological Sciences (EIABS)" conducted by the Department of Biotechnology, School of Bioengineering, SRM Institute of Science and Technology, Kattankulathur, 603 203.

CONFLICTS OF INTEREST

The authors have no conflicts of interest to declare that are relevant to the content of this article.

ETHICAL APPROVALS

This study does not involve experiments on animalsor human subjects.

DATA AVAILABILITY

All data generated and analyzed are included in this research article.

PUBLISHER'S NOTE

This journal remains neutral with regard to jurisdictional claims in published institutional affiliation.

DISCLOSURE STATEMENT

The authors have no commercial, proprietary, or financial interest in the products or companies described in this article.

REFERENCES

Anitha A, Sowmya S, Kumar PS, Deepthi S, Chennazhi KP, Ehrlich H, Tsurkan M, Jayakumar R. Chitin and chitosan in selected biomedical applications. Prog Poly Sci, 2014; 39(9):1644–7.

Al-Rajhi AMH, Yahya R, Abdelghany TM, Fareid MA, Mohamed AM, Amin BH, Masrahi AS. Anticancer, anticoagulant, antioxidant and antimicrobial activities of *Thevetia peruviana* Latex with molecular docking of antimicrobial and anticancer activities. Molecules, 2022; 27(10):3165.

Brentjens R, Saltz L. Islet cell tumors of the pancreas: the medical oncologist's perspective. Surg Clin N Am, 2001; 81(3):527–42.

Das S, Das MP, Das J. Fabrication of porous chitosan/silver nanocomposite film and its bactericidal efficacy against multi-drug resistant (MDR) clinical isolates. J Pharm Res, 2013; 6(1):11–5.

Devi RK. *Cichorium intybus* L. accords hepatoprotection in Streptozotocin induced diabetes mellitus in Wistar rats. Res J Biotechnol, 2018; 13(3):42–5.

Ganeshpurkar A, Saluja AK. The pharmacological potential of rutin. Saudi Pharm J, 2017; 25(2):149–64.

Imani A, Maleki N, Bohlouli S, Kouhsoltani M, Sharifi S, Maleki Dizaj S. Molecular mechanisms of anticancer effect of rutin. Phytother Res, 2021; 35(5):2500–13.

Kim DG, Jeong YI, Choi C, Roh SH, Kang SK, Jang MK, Nah JW. Retinol-encapsulated low molecular water-soluble chitosan nanoparticles. Int J Pharm, 2006; 319(1-2):130–8.

Kopustinskiene DM, Jakstas V, Savickas A, Bernatoniene J. Flavonoids as anticancer agents. Nutrients, 2020; 12(2):457.

Kumar SP, Birundha K, Kaveri K, Devi KR. Antioxidant studies of chitosan nanoparticles containing naringenin and their cytotoxicity effects in lung cancer cells. Int J Biol Macromol, 2015; 78:87–95.

Li X, Deng SJ, Zhu S, Jin Y, Cui SP, Chen JY, Xiang C, Li QY, He C, Zhao SF, Chen HY. Hypoxia-induced lncRNA-NUTF2P3-001 contributes to tumorigenesis of pancreatic cancer by derepressing the miR-3923/KRAS pathway. Oncotarget, 2016; 7(5):6000.

Lobo V, Patil A, Phatak A, Chandra N. Free radicals, antioxidants and functional foods: impact on human health. Pharmacogn Rev, 2010; 4(8):118.

Madesh M, Balasubramanian KA. A microtiter plate assay for superoxide using MTT reduction method. Indian J Biochem Biophys, 1997; 34:535–9.

Mohammed MA, Syeda JT, Wasan KM, Wasan EK. An overview of chitosan nanoparticles and its application in non-parenteral drug delivery. Pharmaceutics, 2017; 9(4):53.

Naskar S, Kuotsu K, Sharma S. Chitosan-based nanoparticles as drug delivery systems: a review on two decades of research. J Drug Target, 2019; 27(4):379–93.

Pan C, Qian J, Zhao C, Yang H, Zhao X, Guo H. Study on the relationship between crosslinking degree and properties of TPP crosslinked chitosan nanoparticles. Carbohydr Polym, 2020; 241:116349.

Panche AN, Diwan AD, Chandra SR. Flavonoids: an overview. J Nutr Sci, 2016; 5:e47.

Patil AG, Jobanputra AH. Rutin-chitosan nanoparticles: fabrication, characterization and application in dental disorders. Polym Plast Technol Eng, 2015; 54(2):202–8.

Perk AA, Shatynska-Mytsyk I, Gerçek YC, Boztaş K, Yazgan M, Fayyaz S, Farooqi AA. Rutin mediated targeting of signaling machinery in cancer cells. Cancer Cell Int, 2014; 14(1):1–5.

Raza ZA, Khalil S, Ayub A, Banat IM. Recent developments in chitosan encapsulation of various active ingredients for multifunctional applications. Carbohydr Res, 2020; 492:108004.

Satari A, Ghasemi S, Habtemariam S, Asgharian S, Lorigooini Z. Rutin: a flavonoid as an effective sensitizer for anticancer therapy; insights into multifaceted mechanisms and applicability for combination therapy. Evid Based Complement Alternat Med, 2021; 2021:9913179.

Sharma A, Boise LH, Shanmugam M. Cancer metabolism and the evasion of apoptotic cell death. Cancers, 2019; 11(8):1144.

Sridevi DV, Devi KTR, Jayakumar N. pH dependent synthesis of TiO2 nanoparticles exerts its effect on bacterial growth inhibition and osteoblasts proliferation. AIP Adv, 2020; 10(9):095119.

Takahashi K, Ota Y, Kogure T, Suzuki Y, Iwamoto H, Yamakita K, Kitano Y, Fujii S, Haneda M, Patel T, Ota T. Circulating extracellular vesicle-encapsulated HULC is a potential biomarker for human pancreatic cancer. Cancer Sci, 2020; 111(1):98–111.

Vernaez O, Neubert KJ, Kopitzky R, Kabasci S. Compatibility of chitosan in polymer blends by chemical modification of bio-based polyesters. Polymers, 2019; 11(12):1939.

Waris G, Ahsan H. Reactive oxygen species: role in the development of cancer and various chronic conditions. J Carcinogen, 2006; 5:14.

Wu Z, He B, He J, Mao X. Upregulation of miR-153 promotes cell proliferation via downregulation of the PTEN tumor suppressor gene in human prostate cancer. Prostate, 2013; 73(6):596–604.

Zhang M, Cao J, Dai X, Chen X, Wang Q. Flavonoid contents and free radical scavenging activity of extracts from leaves, stems, rachis and roots of *Dryopteris erythrosora*. Iran J Pharm Res, 2012; 11(3):991.

How to cite this article:
Devi KTR, Paulraj SJ, Shah Y, Kumar SR, Kejamurthy P. Chitosan-tripolyphosphate nanoparticles encapsulated rutin targeting bacterial growth inhibition and its cytotoxicity on PANC-1 pancreatic adenocarcinoma cell. J Appl Pharm Sci, 2023; 13(04):141–148.